Journal of Hazardous Materials 192 (2011) 1122–1131

Contents lists available at ScienceDirect

Journal of Hazardous Materials

journal homepage: www.elsevier.com/locate/jhazmat

Adsorption of Reactive Red M-2BE dye from water solutions by multi-walled carbon nanotubes and activated carbon

Fernando M. Machado [a], Carlos P. Bergmann [a], Thais H.M. Fernandes [b], Eder C. Lima [b,*], Betina Royer [b], Tatiana Calvete [b], Solange B. Fagan [c]

[a] Department of Material, Federal University of Rio Grande do Sul, Av. Osvaldo Aranha 99, Laboratory 705C, ZIP 90035-190, Porto Alegre, RS, Brazil
[b] Institute of Chemistry, Federal University of Rio Grande do Sul, Av. Bento Gonçalves 9500, Postal Box 15003, ZIP 91501-970, Porto Alegre, RS, Brazil
[c] Department of Nanoscience, UNIFRA, R. dos Andradas 1614, ZIP 97010-032, Santa Maria, RS, Brazil

ARTICLE INFO

Article history:
Received 19 March 2011
Received in revised form 5 June 2011
Accepted 7 June 2011
Available online 14 June 2011

Keywords:
Multi-walled carbon nanotube
Activated carbon
Adsorption
Nonlinear isotherm fitting
Reactive Red M-2BE dye

ABSTRACT

Multi-walled carbon nanotubes and powdered activated carbon were used as adsorbents for the successful removal of Reactive Red M-2BE textile dye from aqueous solutions. The adsorbents were characterised by infrared spectroscopy, N_2 adsorption/desorption isotherms and scanning electron microscopy. The effects of pH, shaking time and temperature on adsorption capacity were studied. In the acidic pH region (pH 2.0), the adsorption of the dye was favourable using both adsorbents. The contact time to obtain equilibrium at 298 K was fixed at 1 h for both adsorbents. The activation energy of the adsorption process was evaluated from 298 to 323 K for both adsorbents. The Avrami fractional-order kinetic model provided the best fit to the experimental data compared with pseudo-first-order or pseudo-second-order kinetic adsorption models. For Reactive Red M-2BE dye, the equilibrium data were best fitted to the Liu isotherm model. Simulated dyehouse effluents were used to check the applicability of the proposed adsorbents for effluent treatment.

1. Introduction

Dyes are one of the most hazardous chemical compound classes found in industrial effluents and need to be treated since their presence in water bodies reduces light penetration, precluding the photosynthesis of aqueous flora [1,2]. They are also aesthetically objectionable for drinking and other purposes [3]. Dyes can cause allergy, dermatitis, skin irritation [4] and also provoke cancer [5] and mutation in humans [6].

The most efficient method for the removal of synthetic dyes from aqueous effluents is the adsorption procedure [7–9]. This process transfers the dyes from the water effluent to a solid phase, thereby keeping the effluent volume to a minimum [10–12]. Subsequently, the adsorbent can be regenerated or stored in a dry place without direct contact with the environment [13].

Different adsorbents have been proposed for the removal of dyes from aqueous solutions [14–20]. Among these, carbon nanotube (CNT) materials have been proposed for the successful removal of dyes from aqueous effluents [21–26]. CNTs have attracted increasing research interest as a new adsorbent [21,22]. They are an attractive alternative for the removal of dye contaminants from aqueous effluents because they have a large specific surface area, small size as well as hollow and layered structures. CNTs have been found to be efficient adsorbents with a capacity that exceeds that of activated carbon [21]. However, up to the best of our knowledge, there are only six papers in the literature, reporting the use of CNTs for dye removal from aqueous effluents [21–26]. Therefore, the use of CNT for dye adsorption requires new studies on this topic.

In the present work, multi-walled carbon nanotubes (MWCNT) were compared with commercial powdered activated carbon (PAC) and these materials were used as adsorbents for the successful removal of Reactive Red M-2BE (RRM) textile dye from aqueous solutions. This dye is largely used for dyeing textiles in the Brazilian cloth industry.

2. Materials and methods

2.1. Solutions

De-ionised water was used throughout the experiments for solution preparation. The textile dye, Reactive Red M-2BE (RRM; C.I. 18214; CAS 23354-52-1; $C_{27}H_{18}N_7O_{16}S_5ClNa_4$; 984.21 g mol^{-1}) was furnished by Dynasty Colourants Co.at 80% purity. The dye was used without further purification. The RRM dye has three sulphonate groups and one sulphato-ethyl-sulphone group (see Supplementary Fig. 1). These groups present negative charges even

* Corresponding author. Tel.: +55 51 3308 7175; fax: +55 51 3308 7304.
E-mail address: profederlima@gmail.com (E.C. Lima).

0304-3894/$ – see front matter © 2011 Elsevier B.V. All rights reserved.
doi:10.1016/j.jhazmat.2011.06.020

Nomenclature

A	Arrhenius constant
C_e	dye concentration at the equilibrium (mg L^{-1})
C_f	dye concentration at ending of the adsorption (mg L^{-1})
C_o	initial dye concentration put in contact with the adsorbent (mg L^{-1})
E_a	activation energy (kJ mol^{-1})
F_{error}	error function
h	the sorption rate (mg g^{-1} h^{-1})
k_{AV}	is the Avrami rate constant (h^{-1})
K	equilibrium adsorption constants of the isotherm fits
K_F	the Freundlich equilibrium constant [mg g^{-1} (L mg^{-1})$^{1/nF}$]
k_f	the pseudo-first order rate constant (h^{-1})
K_L	the Langmuir equilibrium constant (L mg^{-1})
K_g	the Liu equilibrium constant (L mg^{-1})
k_s	the pseudo-second order rate constant (g mg^{-1} h^{-1})
n	number of experiments performed
n_{AV}	is a fractional reaction order (Avrami) which can be related, to the adsorption mechanism
n_F	dimensionless exponent of the Freundlich equation
n_L	dimensionless exponent of the Liu equation
p	number of parameters of the fitted model
q	amount adsorbed of the dye by the adsorbent (mg g^{-1})
q_e	amount adsorbate adsorbed at the equilibrium (mg g^{-1})
$q_{i,model}$	each value of q predicted by the fitted model
$q_{i,exp}$	each value of q measured experimentally
$\bar{q}_{exp}$	average of q measured experimentally
Q_{max}	the maximum adsorption capacity of the adsorbent (mg g^{-1})
q_t	amount of adsorbate adsorbed at time (mg g^{-1})
R	universal gas constant
R^2adj	determination factor
t	time of contact (h)
T	absolute temperature (K)
m	adsorbent mass (g)
V	volume of adsorbate (L)

in highly acidic solutions due to their pKa values lower than zero [27]. The stock solution was prepared by dissolving the dye in distilled water to a concentration of 5.00 g L^{-1}. Working solutions were obtained by diluting the dye stock solutions to the required concentrations. To adjust the pH of the solutions, 0.10 mol L^{-1} sodium hydroxide or hydrochloric acid were used. The pH of the solutions was measured using a Schott Lab 850 set pH meter.

2.2. Adsorbents

MWCNTs with purity of 95% were prepared by catalytic chemical vapour deposition (CCVD). This method of synthesis has been described previously [28]. The PAC was furnished by Merck. Both adsorbents were used without further purification.

The MWCNT and PAC adsorbents were characterized by vibrational spectroscopy in the infrared region with Fourier Transform (FTIR) using a Varian spectrometer, model 640-IR. The spectra were obtained with a resolution of 4 cm^{-1} with 100 cumulative scans.

The surface analyses and porosity were carried out with a volumetric adsorption analyser, Nova 1000, from Quantachrome Instruments, at 77 K (the boiling point of nitrogen). For area and pore calculations, the multi-point BET (Brunauer, Emmett and Teller) and BJH (Barret, Joyner and Halenda) [29] methods were used.

The adsorbent samples were also analysed by scanning electron microscopy (SEM) in a Jeol microscope, model JSM 6060 [30].

The point of zero charge (pH$_{pzc}$) of the adsorbent was determined according to the literature [10,31].

2.3. Adsorption studies

Adsorption studies for the evaluation of the MWCNT and PAC adsorbents for the removal of the RRM dye from aqueous solutions were carried out in triplicate using the batch contact adsorption method. For these experiments, 30.0 mg of adsorbents placed in 50.0 mL cylindrical high-density polypropylene flasks (height 117 mm and diameter 30 mm) containing 20.0 mL of the dye solution (100.0–1000.0 mg L^{-1}) [32], which were agitated for a suitable time (2 min to 6 h in the kinetic experiments; and 1 h in the equilibrium isotherms) at different temperatures (298–323 K). The pH of the dye solutions ranged from 2.0 to 10.0. Subsequently, in order to separate the adsorbents from the aqueous solutions, the flasks were centrifuged at 16,000 rpm for 5 min using a Unicen M Herolab centrifuge (Stuttgart, Germany) in the equilibrium isotherm or filtered in a 0.2 μm membrane in the kinetic experiments, and aliquots of 1–10 mL of the supernatant were properly diluted with an aqueous solution fixed at a suitable pH value.

The final concentrations of the dye which remained in the solution were determined by visible spectrophotometry using a T90+ UV–VIS spectrophotometer furnished by PG Instruments (London-England) provided with quartz optical cells. Absorbance measurements were made at the maximum wavelength of RRM dye at 505 nm.

The amount of dye taken up and the percentage of removal of the dye by the adsorbent were calculated by applying Eqs. (1) and (2), respectively:

$$q = \frac{(C_o - C_r)}{m} \cdot V \quad (1)$$

$$\%\text{Removal} = 100 \cdot \frac{(C_o - C_r)}{C_o} \quad (2)$$

where q is the amount of dye taken up by the adsorbent (mg g^{-1}), C_o is the initial dye concentration put in contact with the adsorbent (mg L^{-1}), C_f is the dye concentration (mg L^{-1}) after the batch adsorption procedure, m is adsorbent mass (g) and V is the volume of the dye solution (L).

The experiments of desorption were carried out according to the procedure: a 200.0 mg L^{-1} of RRM dye was shaken with 50.0 mg of each MWCNT and PAC for 1 h. Then, the loaded adsorbents were filtered in 0.2 μm cellulose acetate and they were firstly washed with water for removing non-adsorbed dye. Then, the dye adsorbed on the adsorbents were agitated with 20.0 mL of: ethanol; n-heptane; n-propanol; methanol; NaOH aqueous solutions (1.0–3.0 mol L^{-1}); and mixture of methanol + NaOH (1.0–7.0 mol L^{-1}) for 15–60 min. The desorbed dye was separated and estimated as described above.

2.4. Kinetic and equilibrium models and its statistical evaluation

The Avrami fractional-order [33], pseudo-first-order [34], pseudo-second-order [35] and intra-particle diffusion [36] kinetic equations are given in Supplementary Table 1. The Langmuir [37], Freundlich [38] and Liu [39] isotherm equations are given in Supplementary Table 2.

The kinetic and equilibrium models were fitted by employing a nonlinear method, with successive interactions calculated by the method of Levenberg-Marquardt. Interactions were also calculated

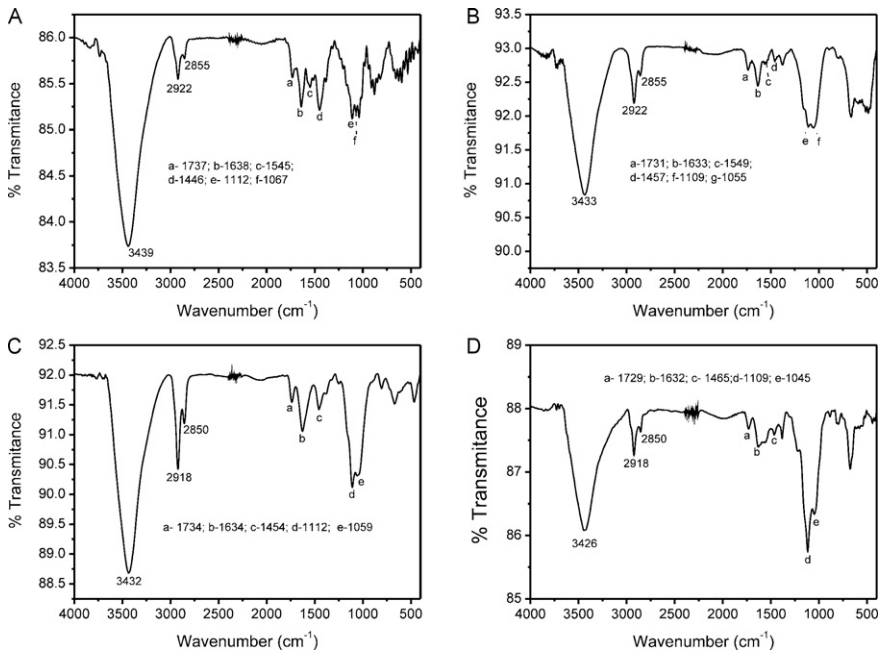

Fig. 1. Infrared spectra of adsorbents: (A) MWCNT; (B) MWCNT + RRM; (C) PAC; (D) PAC + RRM.

by the Simplex method, using the nonlinear fitting facilities of the software Microcal Origin 7.0. In addition, the models were also evaluated by the adjusted determination factor (R^2adj), as well as by an error function (F_{error}) [40] which measured the differences in the amount of dye taken up by the adsorbent predicted by the models and the actual q measured experimentally. $R^2{}_{adj}$ and F_{error} are given below, respectively [40]:

$$R^2_{adj} = \left\{1 - \left[1 - \left(\frac{\sum_i^n (q_{i,\exp} - \bar{q}_{i,\exp})^2 - \sum_i^n (q_{i,\exp} - q_{i,model})^2}{\sum_i^n (q_{i,\exp} - \bar{q}_{i,\exp})^2}\right) \cdot \left(\frac{n-1}{n-p}\right)\right]\right\} \quad (3)$$

$$F_{error} = \sqrt{\left(\frac{1}{n-p} \cdot \sum_i^n (q_{i,\exp} - q_{i,model})\right)^2} \quad (4)$$

where $q_{i,model}$ is each value of q predicted by the fitted model, $q_{i,exp}$ is each value of q measured experimentally, $\bar{q}_{\exp}$ is the average of q measured experimentally, n is the number of experiments performed and p is the number of parameters of the fitted model [40].

2.5. Simulated dyehouse effluent

Two synthetic dyehouse effluents containing five representative reactive dyes used for coloring fibers and their corresponding auxiliary chemicals were prepared in two different pH values, using a mixture of different dyes most often applied to textile fibers industries. According to the practical information obtained from a dyehouse, typically 20% of the reactive dyes and 100% of the dyebath auxiliaries remain in the spent dyebath, and its composition suffer a 5–30-fold dilution during subsequent washing and rinsing stages [10]. The concentrations of the dyes and auxiliary chemicals selected to imitate the exhausted dyebath are given in Supplementary Table 3.

3. Results and discussion

3.1. Characterisation of the adsorbents

The FTIR technique was used to examine the surface groups of adsorbents (MWCNT and PAC) and to identify the groups responsible for dye adsorption. Infrared spectra of the adsorbents and dye-loaded adsorbent samples, before and after the adsorption process, were recorded in the range 4000–400 cm^{-1} (Fig. 1). As previously observed for an activated carbon [41] after the adsorption procedure, the functional groups that interact with the dye suffered a shift to lower wavenumbers when the adsorbate withdrew electrons of the adsorbent group. On the other hand, when the adsorbate furnished electrons to the adsorbent, the FTIR vibration bands shifted to higher wavenumbers [41].

Fig. 1A and B shows the FTIR vibrational spectra of the MWCNT before the adsorption and loaded with the dye RRM (MWCNT + RRM) after the adsorption, respectively. The intense absorption bands at 3439 and 3433 cm^{-1} were assigned to O–H bond stretching, before and after interaction, respectively [41,42] indicating that this group plays a role in the adsorption of the RRM dye. The CH_2 stretching bands at 2922 and 2855 cm^{-1} were assigned to asymmetric and symmetric stretching of CH_2 groups [41,42], respectively, which presented the same wavenumbers before and after adsorption, indicating that these groups did not participate in the adsorption process [32]. Small bands at 1737 and 1731 cm^{-1}, before and after absorption, respectively, were assigned to the carbonyl groups of carboxylic acid [41,42]. Sharp intense peaks observed at 1638 and 1633 cm^{-1}, before and after absorption, respectively, were assigned to the asymmetric carboxylate stretch [42]. The bands at 1545 and 1446 cm^{-1} presented on the MWCNT that were assigned to the aromatic rings modes [42] shifted to higher wavenumbers (1549 and 1457 cm^{-1}, respectively), and also the relative intensity of these bands was remarkably diminished after the adsorption of the RRM dye. These FTIR bands changed after adsorption (Fig. 1B) of the dye, indicating that the mechanism of interaction of the RRM dye with the MWCNT should also occur by the π–π interaction of the dye with the aromatic rings of the carbon nanotube [41], in addition to interactions with other functional groups (OH, COOH). In addition, strong bands ranging from 1112 to 1067 cm^{-1} and 1109 to 1055 cm^{-1} before and after

Table 1
Textural properties of MWCNT and PAC adsorbents.

Adsorbents	Surface area (m^2/g)	Total pore volume (cm^3/g)	Average pore diameter (nm)
MWCNT	180.9	0.345	7.62
PAC	728.7	0.641	3.52

adsorption, respectively, confirmed the presence of a C–O bond (Fig. 1B) [41,42], reinforcing the interaction of the dye with carboxylate groups. Based on the FTIR bands, it could be concluded that the adsorption of RRM dye on MWCNT occurred mainly on the groups OH, COOH and at the aromatic rings.

The vibrational spectra of PAC and dye-loaded PAC adsorbent (PAC + RRM) presented absorption bands at 3432 and 3426 cm^{-1} that were assigned to O–H bond stretching, before (Fig. 1C) and after adsorption (Fig. 1D), respectively [42], indicating that this group plays a role in the adsorption of the RRM dye on the PAC adsorbent. The two CH_2 stretching bands at 2918 and 2850 cm^{-1} were assigned to asymmetric and symmetric stretching of the CH_2 groups, respectively [41,42], which presented the same wavenumbers before and after adsorption, indicating that this group did not participate in the adsorption process, as was also observed for the MWCNT adsorbent. Small bands at 1734 and 1729 cm^{-1}, before and after absorption, respectively, were assigned to the carbonyl groups of carboxylic acid [41,42]. Sharp bands at 1634 cm^{-1} and 1632 cm^{-1} before and after the batch adsorption process, respectively, were assigned to the carboxylate stretch band. It was observed that this band was shifted to lower wavenumbers and that its relative intensity was diminished after adsorption (Fig. 1D) of the dye. Therefore, the mechanism of interaction of the RRM dye with the activated carbon PAC should occur. The band at 1454 cm^{-1} present on the PAC adsorbent that was assigned to the ring mode of the aromatic ring [42] was shifted to higher wavenumbers (1465 cm^{-1}), and the relative intensity of this band was also remarkably diminished after adsorption of the RRM dye. This FTIR band change after adsorption (Fig. 1D) of the dye indicated that the mechanism of interaction of the RRM dye with the PAC adsorbent should also occur by the π–π interaction of the dye with the aromatic rings of the activated carbon [41], as was observed for MWCNT. In addition, strong bands at 1112–1059 and 1109–1045 cm^{-1}, before and after adsorption, respectively, confirmed the presence of a C–O bond (Fig. 1D) [41,42], reinforcing the interaction of the RRM dye with carboxylate groups present on the PAC adsorbent.

By the FTIR results presented in Fig. 1, it can be concluded that the functional groups present on MWCNT were practically the same observed on the PAC adsorbent, where the dye interacted through the OH, COOH and aromatic rings of both carbon adsorbents.

The textural properties of the MWCNT and PAC adsorbents are presented in Table 1. The average pore diameter of MWCNT adsorbent is relatively large, when compared with the activated carbons; this could be attributed to the aggregated pores of MWCNT [43]. Carbon nanotubes form aggregated pores due to the entanglement of tens and hundreds of individual tubes that are adhered to each other as a result of van der Waals forces of attraction [43]. These aggregated pores have the dimensions of a mesopore or higher [43].

The maximum diagonal length of the RRM dye (see Supplementary Fig. 1) is 2.05 nm. The ratios of average pore diameter of the MWCNT and PAC adsorbents to the maximum diagonal length of the dye are 3.7 and 1.7, respectively. Therefore, the mesopores of MWCNT could accommodate up to 3 molecules of RRM and the PAC adsorbent could accommodate only one dye molecule.

Scanning electron microscopy of the adsorbents is presented on Fig. 2. These micrographs suggest that MWCNT could be expanded when immersed in aqueous solution, because this adsorbent is an

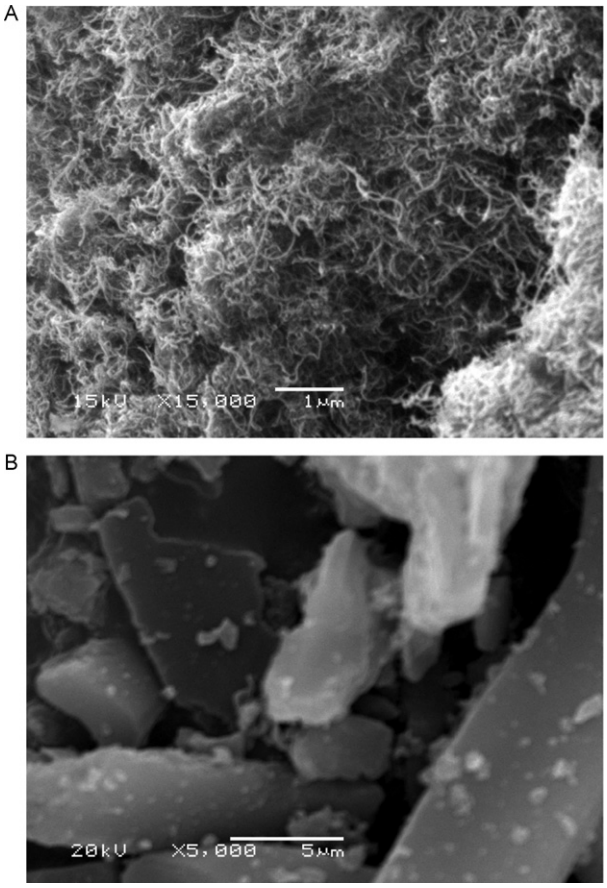

Fig. 2. SEM of adsorbents. (A) MWCNT, magnification 15,000×; (B) PAC, magnification 5000×.

entanglement of carbon tubes [43]. On the other hand, the PAC material is a more compact material, which is composed of carbon fragments [41].

Based on these textural characteristics explained above it is expected that MWCNT would present higher sorption capacity than the PAC for the RRM adsorption, besides of presenting a faster kinetic. This behaviour will be confirmed at Sections 3.3 and 3.4.

3.2. Effects of pH on adsorption

One of the most important factors in adsorption studies is the effect of acidity on the medium [44,45]. Different species may present divergent ranges of suitable pH depending on which adsorbent is used. The effects of initial pH on the percentage of removal of the RRM dye using MWCNT and PAC adsorbents were evaluated within the pH range between 2 and 10 (Fig. 3). For these experiments, all the solutions were prepared keeping the ionic strength fixed with 0.050 mol L^{-1} NaCl solutions. For both adsorbents, the percentage of dye removal decreased from pH 2.0 up to 10.0. For MWCNT and the PAC adsorbent, the decrease in the percentage of dye removal when the pH ranged from 2.0 to 10.0 was 6.87% and 4.23%, respectively.

The pH_{PZC} values determined for MWCNT and PAC adsorbents were 6.85 and 7.30, respectively. For pH values lower than pH_{pzc}, the adsorbent presents a positive surface charge [10,31]. The dissolved RRM dye is negatively charged in water solution, because it possesses three sulphonate groups and one sulphato-ethyl-sulphone group [27]. The adsorption of this dye takes place when the adsorbents present a positive surface charge. For MWCNT and PAC, the electrostatic interaction occurs for pH < 6.85 and 7.30,

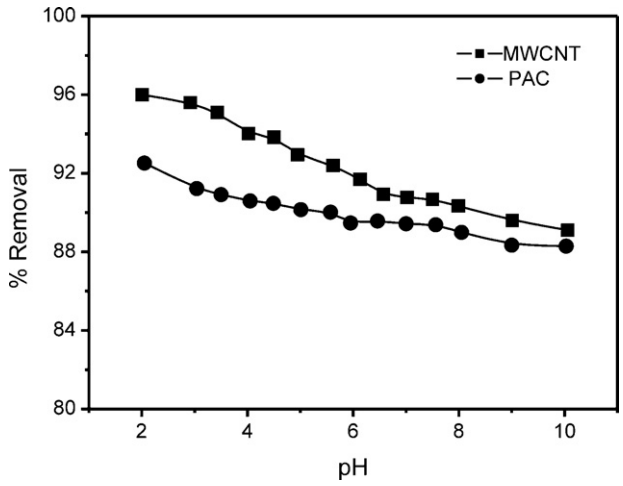

Fig. 3. Effect of pH on the adsorption of RRM dye on MWCNT and PAC. Conditions: C_o 350.0 mg L^{-1} of dye solution; mass of adsorbent of 30.0 mg; the temperature was fixed at 298 K, ionic strength fixed with 0.050 mol L^{-1} NaCl solutions.

respectively. However, the lower the pH value from the pH_{pzc}, the more positive the surface of the adsorbent [10,32]. This behaviour explains the high adsorption capacity of both adsorbents for the RRM dye at pH 2. In order to continue the adsorption studies, the initial pH was fixed at 2.0. It should be stressed that the final pH of the adsorbate solution after the adsorption procedure did not changed remarkably. The final pH values of the adsorbate solutions were measured and its values attained up to 2.2.

3.3. Kinetic studies

Adsorption kinetic studies are important in the treatment of aqueous effluents because they provide valuable information on the mechanism of the adsorption process [45,46].

It is important to point out that the initial RRM concentrations employed during the kinetic studies were relatively high (300.0 and 600.0 mg L^{-1}) when compared with other studies reported in the literature [1–3,16,17,32]. MWCNT and PAC adsorbents have very high adsorption capacities and adsorb practically all the RRM dye when the initial adsorbate concentrations are lower than 150 mg L^{-1}.

In attempting to describe the adsorption kinetics of RRM dye using the MWCNT and PAC adsorbents, three kinetic models were tested, as shown in Fig. 4. The Avrami kinetic parameters are listed in Table 2 for MWCNT and PAC. The pseudo-first order and pseudo-second order kinetic models were not suitably fitted (see Fig. 4) and by this reason these values were not reported on Table 2, because these parameters have no physical meaning. Therefore, the kinetic data were only suitably fitted by the Avrami fractional kinetic model that presented low error function values and also high R^2 values, for the two initial concentrations of the dye using both MWCNT and PAC adsorbents. The pseudo-first-order and pseudo-second-order kinetic model presented F_{error} values of at least 2.9 and 7.9 times higher, respectively, than the values obtained for the Avrami-fractional kinetic adsorption model, using MWCNT adsorbent and 2.4 and 4.8 times higher for pseudo first-order and pseudo-second order, respectively, in relation to Avrami fractional kinetic model for PAC adsorbent. The lower the error function, the lower the difference of the q calculated by the model from the experimentally measured q [9,32,45]. It should be pointed out that the F_{error} utilised in this work took into account the number of the fitted parameters (p term of Eq. (4)), since it has been reported in the literature [47] that, depending on the number of parameters a nonlinear equation presents, it has the best fitting with the results. For this reason, the number of fitted parameters should be considered in the calculation of F_{error}.

In addition, only the Avrami fractional model showed an increase on the kinetic rate constant (k_{AV}) with the increase of temperature from 298 to 323 K. For pseudo-first-order and pseudo-second-order kinetic models, the values for the rate constants did

Table 2
Fractional kinetic parameters for RRM removal using MWCNT and PAC adsorbent. Conditions: pH 2.0; adsorbent mass 30.0 mg.

	298 K	303 K	308 K	313 K	318 K	323 K
MWCNT						
300 mg L^{-1}						
k_{AV} (h^{-1})	6.13	6.68	7.33	7.85	8.59	9.52
q_e (mg g^{-1})	188.5	190.1	189.8	189.9	194.3	190.1
n_{AV}	2.42	2.73	2.30	1.50	1.40	1.15
h (mg g^{-1} h^{-1})	1156.6	1269.5	1391.7	1489.6	1668.9	1810.6
Adjusted R^2	0.9980	0.9997	0.9994	0.9999	0.9998	0.9997
F_{error}	2.94	1.16	1.53	0.697	0.717	0.949
600 mg L^{-1}						
k_{AV} (h^{-1})	6.13	6.66	7.18	7.81	8.47	9.40
q_e (mg g^{-1})	301.2	298.7	295.5	290.6	298.0	290.4
n_{AV}	2.39	2.75	2.20	1.52	1.43	1.20
h (mg g^{-1} h^{-1})	1845.9	1988.8	2121.4	2269.4	2525.6	2728.5
AdjustedR^2	0.9999	0.9997	0.9995	0.9998	0.9998	0.9995
F_{error}	1.24	1.86	2.09	1.30	1.28	1.80
PAC						
300 mg L^{-1}						
k_{AV} (h^{-1})	5.19	5.83	6.69	7.85	9.30	10.5
q_e (mg g^{-1})	118.4	119.3	119.8	119.7	120.0	120.4
n_{AV}	1.96	2.11	2.03	1.95	1.90	0.857
h (mg g^{-1} h^{-1})	615.0	695.9	801.5	939.8	1115.3	1268.8
Adjusted R^2	0.9997	0.9993	0.9997	0.9998	0.9997	0.9994
F_{error}	0.736	1.09	0.685	0.537	0.601	0.803
600 mg L^{-1}						
k_{AV} (h^{-1})	5.24	5.80	6.67	7.78	8.87	10.1
q_e (mg g^{-1})	221.5	222.2	236.2	235.9	237.6	238.2
n_{AV}	1.99	2.03	1.99	1.93	1.84	1.06
h (mg g^{-1} h^{-1})	1159.3	1288.3	1575.2	1836.4	2107.0	2396.9
Adjusted R^2	0.9999	0.9999	0.9998	0.9998	0.9999	0.9990
F_{error}	0.910	0.928	1.22	0.940	0.632	2.05

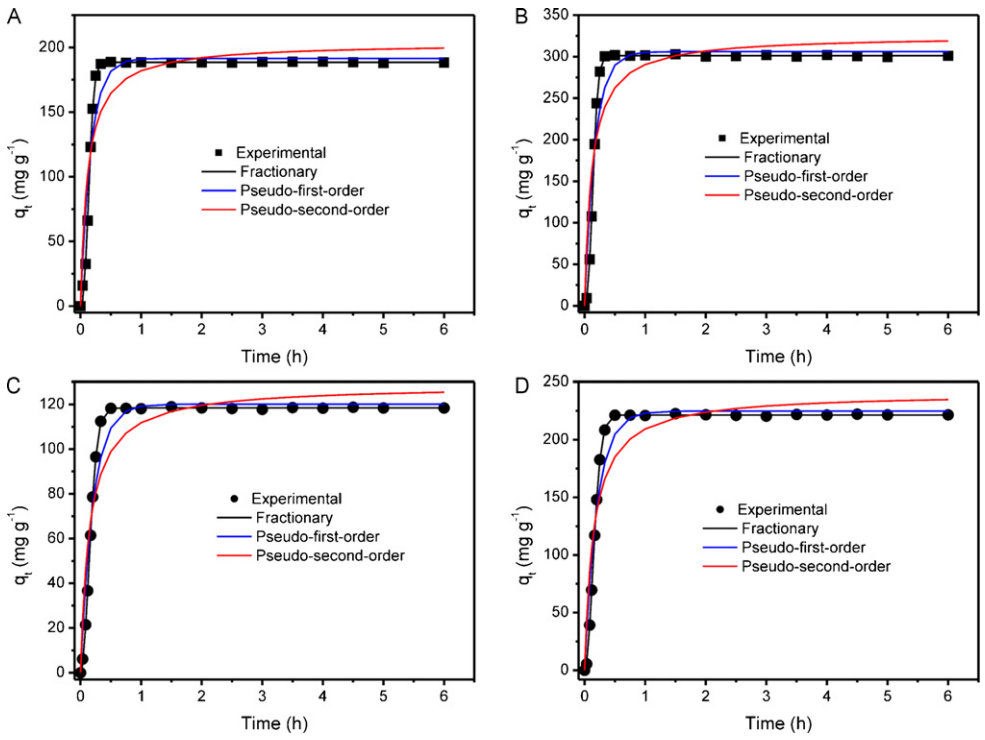

Fig. 4. Kinetic adsorption curves for RRM uptake at 298 K on MWCNT: (A) C_o 300 mg L^{-1}; (B) C_o 600 mg L^{-1}; and on PAC: (C) C_o 300 mg L^{-1}; (D) and C_o 600 mg L^{-1}. Conditions: pH 2.0; mass of adsorbent 30.0 mg.

not follow a regular pattern. Taking into account that the F_{error} values obtained by pseudo-first-order and pseudo-second-order kinetic models were a little bit higher than the values obtained with the Avrami fractional model, it can be inferred that this kinetic model should better explain the adsorption kinetics of RRM on MWCNT and PAC adsorbents.

The rate constant of the Avrami fractional model could be expressed as a function of temperature by the Arrhenius relationship using Eq. (5) [48,49]:

$$Lnk_{AV} = LnA - \frac{Ea}{RT} \quad (5)$$

where k_{AV} is the fractional Avrami constant rate (h^{-1}), A is the Arrhenius constant, E_a is the activation energy (kJ mol^{-1}), R is the universal gas constant (8.314 J K^{-1} mol^{-1}) and T is the absolute temperature (K). The activation energy can be calculated from the slope of a plot of $Ln(k_{AV})$ versus $1/T$ (see supplementary Fig. 2).

For the adsorption of RRM dye on the MWCNT adsorbent, the values of activation energy calculated according to the Arrhenius plot were 13.8 and 13.4 kJ mol^{-1} for initial RRM dye concentrations of 300 and 600 mg L^{-1}, respectively. For the adsorption of RRM dye on the PAC adsorbent, the values of activation energy were 23.3 and 21.5 kJ mol^{-1}, for RRM initial concentrations of 300 and 600 mg L^{-1} (see supplementary Fig. 2). Considering the values of activation energy of RRM obtained with MWCNT and PAC adsorbents, it can be concluded that the kinetics of adsorption of the dye on MWCNT is much faster when compared to the PAC adsorbent. This faster kinetics of adsorption of RRM dye on MWCNT could be attributed to the textural properties of the carbon nanotube, where the aggregated pores could be expanded when immersed in an aqueous solution, increasing the volume of the aggregated pores. On the other hand, the activated carbon is a more compact material which presents pores that do not expand when in contact with the RRM dye solution.

3.4. Equilibrium studies, desorption and mechanism of adsorption

An adsorption isotherm describes the relationship between the amount of adsorbate taken up by the adsorbent (q_e) and the adsorbate concentration remaining in the solution after the system has attained equilibrium (C_e). In this work, the Langmuir [37], the Freundlich [38] and the Liu [39] isotherm models were tested.

The isotherms of adsorption were carried out from 298 to 323 K with RRM dye on the two adsorbents and were performed using the best experimental conditions previously described (see Fig. 5). Based on the F_{error}, the Liu model was the best isotherm model for both adsorbents at all the six temperatures studied. The Liu model showed (Table 3) the lowest F_{error} values, which means that the q fit by the isotherm model was close to the q measured experimentally. The Langmuir and the Freundlich isotherm models were not suit-

Table 3
Liu isotherm parameters for RRM adsorption, using MWCNT and PAC as adsorbents. Conditions: adsorbent mass of 30.0 mg; pH fixed at 2.0, contact time 1 h.

	MWCNT						PAC					
	298 K	303 K	308 K	313 K	318 K	323 K	298 K	303 K	308 K	313 K	318 K	323 K
Q_{max} (mg g^{-1})	312.3	319.2	325.1	327.8	330.0	335.7	243.9	246.5	249.6	252.2	255.1	260.7
K_g (L mg^{-1})	0.1179	0.1434	0.1803	0.2215	0.2692	0.3303	0.6315	0.8395	1.120	1.470	1.956	2.537
n_L	1.20	0.866	0.698	0.565	0.604	0.477	0.709	0.638	1.25	1.05	1.08	0.441
R^2	0.9999	0.9998	0.9999	0.9998	0.9999	1.000	0.9999	0.9998	0.9994	0.9996	0.9996	0.9999
F_{error}	0.2321	0.4146	0.3265	0.3364	0.2817	0.3029	0.3111	0.5375	0.5520	0.4529	0.5569	0.09022

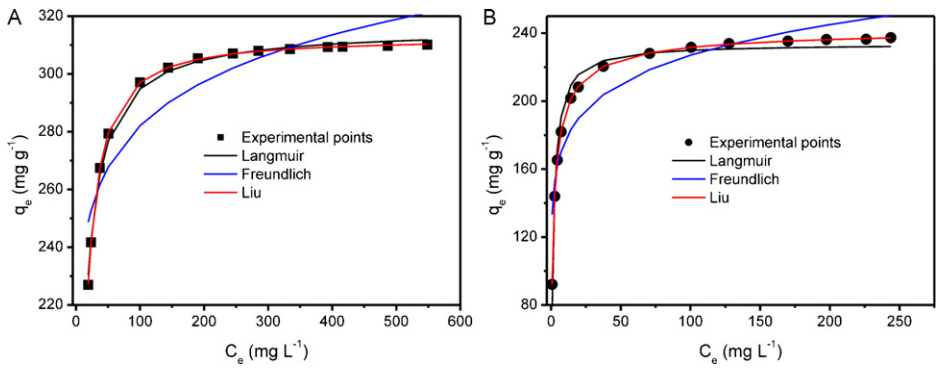

Fig. 5. Isotherm curves of RRM adsorption at 298 K on (A) MWCNT and (B) PAC. Conditions: pH was fixed at 2.0; the adsorbent mass was fixed at 30 mg; the contact time was fixed at 1 h.

ably fitted, presenting F_{error} values ranging from 3.77 to 56.4-fold and from 2.31 to 54.1-fold higher than the F_{error} values obtained by the Liu isotherm model, using MWCNT and PAC as adsorbents, respectively. By this reason, the isotherm parameters of the Langmuir and the Freundlich were not presented on Table 3 because these values have no physical meaning.

The maximum amounts of RRM uptake were 335.7 and 260.7 mg g^{-1} for MWCNT and PAC, respectively. These values indicate that these adsorbents are very good adsorbents for RRM removal from aqueous solutions.

Taking into account that is difficult to compare the sorption capacities of the dyes with different adsorbents, since the dyes reported in the literature are given as commercial dyes, and also considering that the same dye could present different commercial trade names depending on its manufacturer, in Table 4 [1–3,10,13,16,17,24,32,41,44,50–52] is presented a comparison of sorption capacities of different dyes adsorbed in different adsorbents. Based on the Table 4 both MWCNT and PAC adsorbents presented good sorption capacities when compared with the adsorption of different dyes on different adsorbents.

It should be highlighted that the maximum amount adsorbed of RRM dye on MWCNT was 28.8% higher than the value obtained on PAC. The textural characteristics of MWCNT discussed in Section 3.1 explain this difference.

A mechanism for adsorption of RRM on MWCNT is proposed (see Fig. 6). In the first step, the MWCNT is immersed in a solution with pH < pH_{pzc} (pH 2.0), being the functional groups (OH, carboxylates, please see Fig. 1) of the adsorbent protonated (see Fig. 3). This step is fast. The second step is the separation of the agglomerates of dyes in the aqueous solution. Dyes are in an organized state in the aqueous solution, besides being hydrated [32]. These self-associations of dyes in aqueous solutions should be dissociated before these dyes being adsorbed. Furthermore, the dyes should be dehydrated before being adsorbed. For RRM dye, this step is relatively fast. The third stage is the electrostatic attraction of the negatively charged dyes by the positively surface charged MWCNT adsorbent at pH 2. This stage should be the rate controlling step.

3.5. Thermodynamic studies

Thermodynamic parameters related to the adsorption process, i.e., Gibb's free energy change (ΔG°, kJ mol^{-1}), enthalpy change (ΔH°, kJ mol^{-1}) and entropy change (ΔS°, J mol^{-1} K^{-1}) are determined by the following equations:

$$\Delta G\circ = \Delta H \circ - T\Delta S\circ \quad (6)$$

$$\Delta G\circ = -RTLn(K) \quad (7)$$

The combination of Eqs. (6) and (7), gives:

$$Ln(K) = \frac{\Delta S\circ}{R} - \frac{\Delta H\circ}{R} \times \frac{1}{T} \quad (8)$$

where R is the universal gas constant (8.314 J K^{-1} mol^{-1}), T is the absolute temperature (Kelvin) and K represents the equilibrium adsorption constants of the isotherm fits. It has been reported in the literature that different adsorption equilibrium constants (K) were obtained from different isotherm models [9,10,13,17,41,53–57]. Thermodynamic parameters of adsorption can be estimated from

Table 4
Comparison of maxima adsorption capacities of different dyes using different adsorbents. The values were obtained at the best experimental conditions of each work.

Adsorbent	Dye adsorbate	Q_{max} (mg g^{-1})	Ref.
Brazilian pine-fruit shell	Reactive Red 194	20.8	1
Brazilian pine-fruit shell	Methylene blue	252	2
3-trimethoxysilylpropylurea grafted on octosilicate Na-RUB-18	Reactive Black 5	76.8	3
Activated carbon prepared from Brazilian pine-fruit shell (physical activation)	Reactive Red 120	275	10
Activated carbon prepared from Brazilian pine-fruit shell (chemical activation)	Basic Green 1	219	13
OrganofunctionalizedKenyaite	Sumifix Brilliant Orange 3R	70.7	16
1,4-diazoniabicyclo[2.2.2]octane grafted silica gel	direct yellow 4	57.3	17
Multi-wall-carbon nanotube (MWCNT)	Congo Red	140.1	24
Multi-wall-carbon nanotube (MWCNT)	Reactive green HE4BD	151.9	24
Multi-wall-carbon nanotube (MWCNT)	Golden yellow MR	141.6	24
Cupuassu shell	Reactive Red 194	64.1	32
Cupuassu shell	Direct Blue 53	37.5	32
Activated carbon prepared from Brazilian pine-fruit shell (chemical activation)	Remazol Black B	74.6	41
Acidic magadiite	Methylene Blue	174	44
Iron complex of lignin	Brilliant Red 2BE	73.6	50
chitosan hydrogel beads coated on multiwall carbon nanotube	Congo Red	200	51
clay minerals of halloysite nanotubes (HNTs)	Methyl violet	113.6	52
Powered activatec carbon (PAC)	Reactive Red M-2BE	260.7	This worrk
Multi wall carbon nanotube (MWCNT)	Reactive Red M-2BE	335.7	This worrk

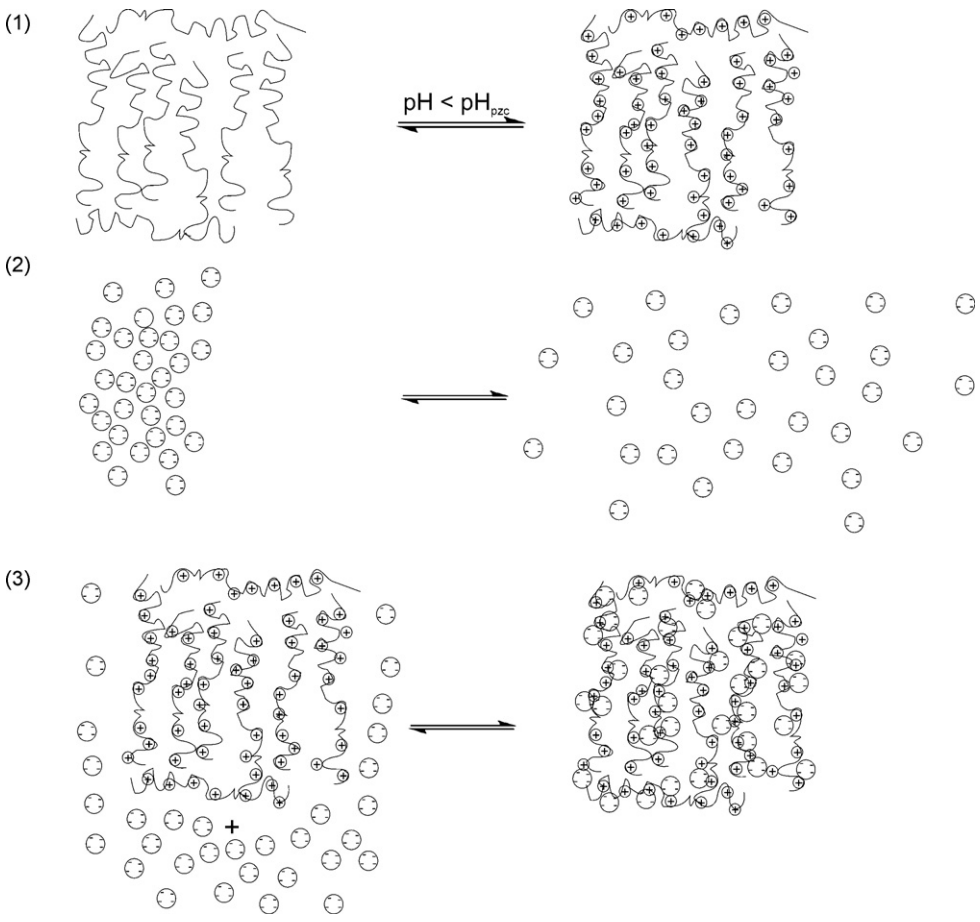

Fig. 6. Mechanism of adsorption of RRM on MWCNT.

the K_g (Liu equilibrium constant), as already reported in the literature [9,10,13,17,41].

The ΔH° and ΔS° values can be calculated from the slope and intercept of the linear plot of $Ln(K)$ versus $1/T$.

The thermodynamic results are depicted in Supplementary Table 4. The R^2 values of the linear fit were at least 0.999 indicating that the values of enthalpy and entropy calculated for both adsorbents were confident. In addition, the magnitude of enthalpy was consistent with an electrostatic interaction of an adsorbent with an adsorbate [22], reinforcing the mechanism suggested at Fig. 6. The kind of interaction can be classified, to a certain extent, by the magnitude of enthalpy change. Physisorption, such as van der Waals interactions, are usually lower than 20 kJ mol^{-1}. Electrostatic interaction ranges from 20 to 80 kJ mol^{-1} and these kind of interactions are, frequently, classified as physisorption [22]. Chemisorption bond strengths can be 80–450 kJ mol^{-1} [22]. Enthalpy changes (ΔH°) indicate that the adsorption followed endothermic processes. Negative values of ΔG indicate that the RRM reactive dye adsorption by MWCNT and PAC adsorbents was a spontaneous and favourable process for all the studied temperatures. The positive values of ΔS° confirmed a high preference of RRM molecules on the carbon surface of MWCNT and PAC, and also suggested the possibility of some structural changes or readjustments in the dye-carbon adsorption complex [58]. Besides, it is consistent with the dehydration of a dye molecule before its adsorption to carbon surface, and the release of these water molecules to the bulk solution, as also commented in the suggested mechanism discussed in Fig. 6. The increase in the adsorption capacities of MWCNT and PAC at higher temperatures may be attributed to the enhanced mobility and penetration of dye molecules within the adsorbent porous structures by overcoming the activation energy barrier and enhancing the rate of intra-particle diffusion [58].

3.6. Treatment of a simulated dyehouse effluent

In order to verify the efficiency of the MWCNT and PAC as adsorbents for removal of dyes from textile effluents, simulated dyehouse effluents were prepared (see Supplementary Table 3). The UV–VIS spectra of the untreated effluents (pH 2.0 and 5.0) and treated with MWCNT and PAC were recorded from 350 to 800 nm (Fig. 7). The area under the absorption bands from 350 to 800 nm were utilized to monitor the percentage of dyes mixture removed from the simulated dye effluents. The MWCNT adsorbent removed 99.8% (Fig. 7A) of the dye mixture at pH 2.0 and 98.7% at pH 5.0 (Fig. 7B). The PAC adsorbent removed 87.6% (Fig. 7A) of the dye mixture at pH 2.0 and 90.8% at pH 5.0 (Fig. 7B). The efficiency of MWCNT adsorbent for treating a simulated dyehouse effluent presented a slightly better performance at two different pH values when compared with PAC adsorbent. This result is in agreement with the previous results obtained in this work (please see Section 3.4). However the PAC adsorbent presented a slightly lower performance for treating a simulated dyehouse effluent, it can be used as well as MWCNT for real textile wastewater treatment (see Supplementary Fig. 3).

3.7. Desorption experiments

In order to check the reuse of the MWCNT and PAC as adsorbents for the adsorption of RRM dye, desorption experiments were carried-out. Several eluents such as, ethanol; n-heptane; n-

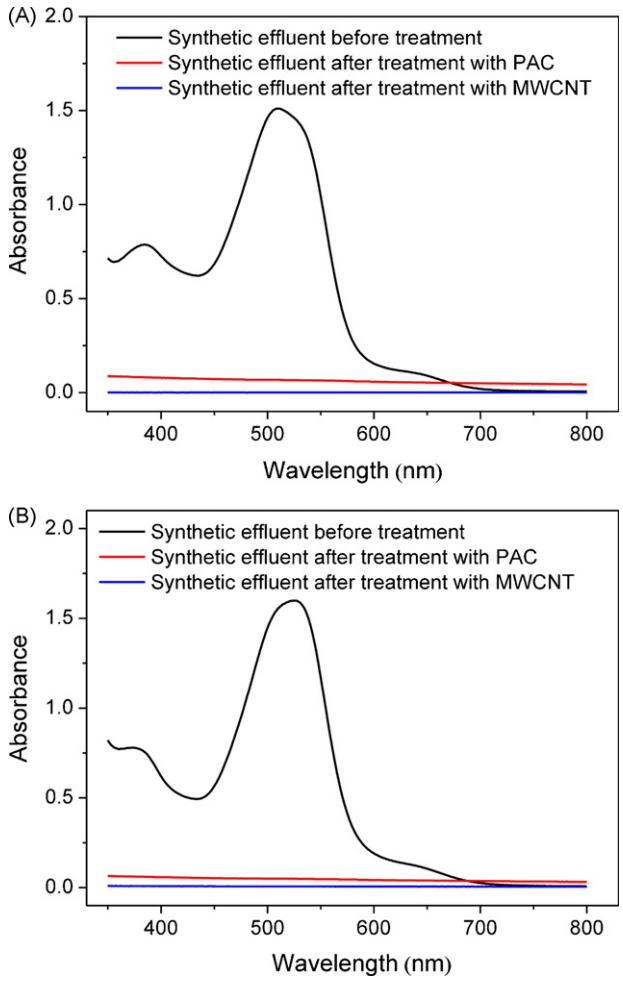

Fig. 7. UV–VIS spectra of simulated dye effluents before and after adsorption treatment with PAC and MWCNT. (A) pH 2.0; (B) pH 5.0. The temperature was fixed at 298 K.

propanol; methanol; NaOH aqueous solutions (1.0–3.0 mol L^{-1}); and mixture of methanol + NaOH (1.0–7.0 mol L^{-1}) were tested for regeneration of the loaded adsorbent (see Table 5). For MWCNT, it should be mentioned that the mixture of methanol + aqueous solutions of NaOH (1.0–7.0 mol L^{-1})desorbed the dye uptaken by the adsorbent immediately, on the other hand, the recoveries of the adsorbent using aqueous NaOH of different concentrations as regenerating solutions did not occurred efficiently even after 1 h of agitation (recoveries <9%). The organic solvents such as ethanol, methanol, n-propanol and n-heptane were also not efficient for the dye desorption from MWCNT (recoveries <14%). The best elution efficiency was obtained with the mixture methanol + 4.0 mol L^{-1} NaOH. This result confirms the FTIR results and the pH studies described above. The RRM dye at pH 2.0 is attracted electrostatically by the MWCNT. This interaction was corrupted with the NaOH solution. However, besides this electrostatic interaction, there are also some interactions between the aromatic groups present on the MWCNT with the aromatic rings of the dye. For breaking this interaction, it was required methanol to improve the elution efficiency (which attained up to 87.5% with the mixture methanol + 4.0 mol L^{-1} NaOH). For PAC adsorbent, the elution efficiency was lower than 12% for all the eluents tested, indicating that activated carbons could not be reutilized for adsorption purposes. On the other hand the MWCNT, eluted with the mixture methanol + 4.0 mol L^{-1} was reutilized for the adsorption of the RRM dye, attaining a sorption efficiency of about 83% in the second cycle, 80% in the third cycle and 78% at the fourth cycle of adsorption/desorption when compared with the first cycle of adsorption/desorption. Therefore, the use of MWCNT for dye adsorption could be economically viable since it allows its regeneration. In addition, there is a tendency for decreasing the prices of CNT with their industrial production growth in the last years [59].

Table 5
Desorption of RRM dye loaded on MWCNT and PACadsorbents. Conditions for adsorption: initial RRM concentration 200 mg L^{-1}; mass of adsorbent 50.0 mg, pH 2.0; time of contact 1 h.

Conditions for desorption	% Desorption	
	MWCNT	PAC
Ethanol	13.74	11.6
n-heptane	0.50	0.20
n-propanol	12.54	11.97
Methanol	10.96	9.70
1.0 mol L^{-1} NaOH (aqueous solution)	6.45	4.35
2.0 mol L^{-1} NaOH (aqueous solution)	7.52	4.53
3.0 mol L^{-1} NaOH (aqueous solution)	8.63	4.67
Methanol + 1.0 mol L^{-1} NaOH	20.61	2.25
Methanol + 2.0 mol L^{-1} NaOH	35.58	2.54
Methanol + 3.0 mol L^{-1} NaOH	65.56	2.94
Methanol + 4.0 mol L^{-1} NaOH	87.50	2.57
Methanol + 5.0 mol L^{-1} NaOH	75.35	3.31
Methanol + 6.0 mol L^{-1} NaOH	56.36	3.14
Methanol + 7.0 mol L^{-1} NaOH	32.25	2.94

4. Conclusions

Multi-wall carbon nanotube (MWCNT) and powdered activated carbon (PAC) were good adsorbents to remove Reactive Red M-2BE (RRM) textile dye from aqueous solutions. The adsorbent materials were characterised by FTIR spectroscopy, SEM and N_2 adsorption/desorption curves.

The RRM dye interacted with the MWCNT and PAC adsorbents at the solid/liquid interface when suspended in water. The best conditions were established with respect to pH and contact time to saturate the available sites located on the adsorbent surface. Three kinetic models were used to adjust the adsorption, and the best fit was the Avrami fractional kinetic model. The activation energy of the adsorption process was calculated by performing kinetic analysis at different temperatures (298–323 K). The equilibrium isotherm of the RRM dye was obtained, and these data fit best to the Liu isotherm model. The maximum adsorption capacities were 335.7 and 260.7 mg g^{-1} for MWCNT and PAC, respectively. The thermodynamic parameters of adsorption (ΔH°; ΔS° and ΔG) were calculated. For treatment of simulated industrial textile effluents, the MWCNT adsorbent presented very good performance for removing at least 98.7% of the mixture of dyes in a medium containing high saline concentrations. The MWCNT material loaded with RRM dye could be regenerated efficiently using a mixture methanol + 4 mol L^{-1} NaOH.

Acknowledgements

The authors are grateful to CNPq, and to FAPERGS for financial support and fellowships.

Appendix A. Supplementary data

Supplementary data associated with this article can be found, in the online version, at doi:10.1016/j.jhazmat.2011.06.020.

References

[1] E.C. Lima, B. Royer, J.C.P. Vaghetti, N.M. Simon, B.M. da Cunha, F.A. Pavan, E.V. Benvenutti, R.C. Veses, C. Airoldi, Application of Brazilian-pine fruit coat as a

biosorbent to removal of Reactive Red 194 textile dye from aqueous solution, kinetics and equilibrium study, J. Hazard. Mater. 155 (2008) 536–550.
[2] B. Royer, N.F. Cardoso, E.C. Lima, J.C.P. Vaghetti, N.M. Simon, T. Calvete, R.C. Veses, Applications of Brazilian-pine fruit shell in natural and carbonized forms as adsorbents to removal of methylene blue from aqueous solutions – kinetic and equilibrium study, J. Hazard. Mater. 164 (2009) 1213–1222.
[3] B. Royer, N.F. Cardoso, E.C. Lima, T.R. Macedo, C. Airoldi, A useful organofunctionalized layered silicate for textile dye removal, J. Hazard. Mater. 181 (2010) 366–374.
[4] D.S. Brookstein, Factors associated with textile pattern dermatitis caused by contact allergy to dyes, finishes, foams, and preservatives, Dermatol. Clin. 27 (2009) 309–322.
[5] R.O.A. de Lima, A.P. Bazo, D.M.F. Salvadori, C.M. Rech, D.P. Oliveira, G.A. Umbuzeiro, Mutagenic and carcinogenic potential of a textile azo dye processing plant effluent that impacts a drinking water source, Mutat. Res. Genet. Toxicol. Environ. Mutagen. 626 (2007) 53–60.
[6] P.A. Carneiro, G.A. Umbuzeiro, D.P. Oliveira, M.V.B. Zanoni, Assessment of water contamination caused by a mutagenic textile effluent/dyehouse effluent bearing disperse dyes, J. Hazard. Mater. 174 (2010) 694–699.
[7] J.J.M. Órfão, A.I.M. Silva, J.C.V. Pereira, S.A. Barata, I.M. Fonseca, P.C.C. Faria, M.F.R. Pereira, Adsorption of a reactive dye on chemically modified activated carbons-influence of pH, J. Colloid Interface Sci. 296 (2006) 480–489.
[8] M. Olivares-Marín, V. Del-Prete, E. Garcia-Moruno, C. Fernández-González, A. Macías-García, V. Gómez-Serrano, The development of an activated carbon from cherry stones and its use in the removal of ochratoxin A from red wine, Food Control. 20 (2009) 298–303.
[9] T. Calvete, E.C. Lima, N.F. Cardoso, J.C.P. Vaghetti, S.L.P. Dias, F.A. Pavan, Application of carbon adsorbents prepared from Brazilian-pine fruit shell for the removal of reactive orange 16 from aqueous solution: kinetic, equilibrium, and thermodynamic studies, J. Environ. Manage. 91 (2010) 1695–1706.
[10] T. Calvete, E.C. Lima, N.F. Cardoso, S.L.P. Dias, F.A. Pavan, Application of carbon adsorbents prepared from the Brazilian-pine fruit shell for removal of Procion Red MX 3B from aqueous solution – kinetic, equilibrium, and thermodynamic studies, Chem. Eng. J. 155 (2009) 627–636.
[11] E.M. Cuerda-Correa, J.R. Domínguez-Vargas, F.J. Olivares-Marín, J.B. de Heredia, On the use of carbon blacks as potential low-cost adsorbents for the removal of non-steroidal anti-inflammatory drugs from river water, J. Hazard. Mater. 177 (2010) 1046–1053.
[12] R. Malarvizhi, Y.S. Ho, The influence of pH and the structure of the dye molecules on adsorption isotherm modeling using activated carbon, Desalination 264 (2010) 97–101.
[13] T. Calvete, E.C. Lima, N.F. Cardoso, S.L.P. Dias, E.S. Ribeiro, Removal of brilliant green dye from aqueous solutions using home made activated carbons, Clean Soil Air Water 38 (2010) 521–532.
[14] S. Rosa, M.C.M. Laranjeira, H.G. Riela, V.T. Fávere, Cross-linked quaternary chitosan as an adsorbent for the removal of the reactive dye from aqueous solutions, J. Hazard. Mater. 155 (2008) 253–260.
[15] A. Afkhami, M. Saber-Tehrani, H. Bagheri, Modified maghemite nanoparticles as an efficient adsorbent for removing some cationic dyes from aqueous solution, Desalination 263 (2010) 240–248.
[16] B. Royer, N.F. Cardoso, E.C. Lima, V.S.O. Ruiz, T.R. Macedo, C. Airoldi, Organofunctionalized kenyaite for dye removal from aqueous solution, J. Colloid Interface Sci. 336 (2009) 398–405.
[17] D.S.F. Gay, T.H.M. Fernandes, C.V. Amavisca, N.F. Cardoso, E.V. Benvenutti, T.M.H. Costa, E.C. Lima, Silica grafted with a silsesquioxane containing the positively charged 1 4-diazoniabicyclo[2. 2. 2]octane group used as adsorbent for anionic dye removal, Desalination 258 (2010) 128–135.
[18] F. Zermane, O. Bouras, M. Baudu, J.P. Basly, Cooperative coadsorption of 4-nitrophenol and basic yellow 28 dye onto an iron organo–inorgano pillared montmorillonite clay, J. Colloid Interface Sci. 350 (2010) 315–319.
[19] M. Greluk, Z. Hubicki, Kinetics, isotherm and thermodynamic studies of Reactive Black 5 removal by acid acrylic resins, Chem. Eng. J. 162 (2010) 919–926.
[20] H.Y. Zhu, R. Jiang, L. Xiao, Adsorption of an anionic azo dye by chitosan/kaolin/γ-Fe_2O_3 composites, Appl. Clay Sci. 48 (2010) 522–526.
[21] C. Wu, Adsorption of reactive dye onto carbon nanotubes: equilibrium, kinetics and thermodynamics, J. Hazard. Mater. 144 (2007) 93–100.
[22] C.Y. Kuo, C.H. Wu, J.Y. Wu, Adsorption of direct dyes from aqueous solutions by carbon nanotubes: determination of equilibrium, kinetics and thermodynamics parameters, J. Colloid Interface Sci. 327 (2008) 308–315.
[23] J.L. Gong, B. Wang, G.M. Zeng, C.P. Yang, C.G. Niu, Q.Y. Niu, W.J. Zhou, Y. Liang, Removal of cationic dyes from aqueous solution using magnetic multi-wall carbon nanotube nanocomposite as adsorbent, J. Hazard. Mater. 164 (2009) 1517–1522.
[24] A.K. Mishra, T. Arockiadoss, S. Ramaprabhu, Study of removal of azo dye by functionalized multi walled carbon nanotubes, Chem. Eng. J. 162 (2010) 1026–1034.
[25] G.P. Hao, W.C. Li, S. Wang, S. Zhang, A.H. Lu, Tubular structured ordered mesoporous carbon as an efficient sorbent for the removal of dyes from aqueous solutions, Carbon 48 (2010) 3330–3339.
[26] Y. Yao, F. Xu, M. Chen, Z. Xu, Z. Zhu, Adsorption behavior of methylene blue on carbon nanotubes, Bioresour. Technol. 101 (2010) 3040–3046.
[27] J.D. Roberts, M.C. Caserio, Basic Principles of Organic Chemistry, second ed., W.A. Benjamin Incorporation, London, 1977.
[28] M. Bierdel, S. Buchholz, V. Michele, L. Mleczko, R. Rudolf, M. Voetz, A. Wolf, Industrial production of multiwalled carbon nanotubos, Phys. Status Solidi (B) 244 (2007) 3939–3943.
[29] L.T. Arenas, E.C. Lima, A.A. dos Santos-Jr, J.C.P. Vaghetti, T.M.H. Costa, E.V. Benvenutti, Use of statistical design of experiments to evaluate the sorption capacity of 1 4-diazoniabicycle[2. 2. 2]octane/silica chloride for Cr(VI) adsorption, Colloids Surf. A 297 (2007) 240–248.
[30] J.C.P. Vaghetti, E.C. Lima, B. Royer, J.L. Brasil, B.M. da Cunha, N.M. Simon, N.F. Cardoso, C.P.Z. Noreña, Application of Brazilian-pine fruit coat as a biosorbent to removal of Cr(VI) from aqueous solution. Kinetics and equilibrium study, Biochem. Eng. J. 42 (2008) 67–76.
[31] A.E. Ofomaja, Y.S. Ho, Effect of pH on cadmium biosorption by coconut copra meal, J. Hazard. Mater. 139 (2007) 356–362.
[32] N.F. Cardoso, E.C. Lima, I.S. Pinto, C.V. Amavisca, B. Royer, R.B. Pinto, W.S. Alencar, S.F.P. Pereira, Application of cupuassu shell as biosorbent for the removal of textile dyes from aqueous solution, J. Environ. Manage. 92 (2011) 1237–1247.
[33] E.C.N. Lopes, F.S.C. dos Anjos, E.F.S. Vieira, A.R. Cestari, An alternative Avrami equation to evaluate kinetic parameters of the interaction of Hg(II) with thin chitosan membranes, J. Colloid Interface Sci. 263 (2003) 542–547.
[34] S. Largegren, About the theory of so-called adsorption of soluble substances, K. Sven. Vetenskapsakad. Handl. 24 (1898) 1–39.
[35] Y.S. Ho, G.M. Mckay, Pseudo-second order model for sorption process, Process Biochem. 34 (1999) 451–465.
[36] W.J. Weber Jr., J.C. Morris, Kinetics of adsorption on carbon from solution, J. Sanit. Eng. Div. Am. Soc. Civil Eng. 89 (1963) 31–59.
[37] I. Langmuir, The adsorption of gases on plane surfaces of glass, mica and platinum, J. Am. Chem. Soc. 40 (1918) 1361–1403.
[38] H. Freundlich, Adsorption in solution, Phys. Chem. Soc. 40 (1906) 1361–1368.
[39] Y. Liu, H. Xu, S.F. Yang, J.H. Tay, A general model for biosorption of Cd^{2+}, Cu^{2+} and Zn^{2+} by aerobic granules, J. Biotechnol. 102 (2003) 233–239.
[40] E.C. Lima, B. Royer, J.C.P. Vaghetti, J.L. Brasil, N.M. Simon, A.A. dos Santos-Jr, F.A. Pavan, S.L.P. Dias, E.V. Benvenutti, E.A. da Silva, Adsorption of Cu(II) on Araucaria angustifolia wastes: determination of the optimal conditions by statistic design of experiments, J. Hazard. Mater. 140 (2007) 211–220.
[41] N.F. Cardoso, R.B. Pinto, E.C. Lima, T. Calvete, C.V. Amavisca, B. Royer, M.L. Cunha, T.H.M. Fernandes, I.S. Pinto, Removal of remazol black B textile dye from aqueous solution by adsorption, Desalination 269 (2011) 92–103.
[42] B. Smith, Infrared Spectral Interpretation. A Systematic Approach, CRC Press, Boca Raton, 1999.
[43] V.K.K. Upadhyayula, S. Deng, M.C.G.B. Mitchell, Smith application of carbon nanotube technology for removal of contaminants in drinking water: a review, Sci. Total Environ. 408 (2009) 1–13.
[44] B. Royer, N.F. Cardoso, E.C. Lima, T.R. Macedo, C. Airoldi, Sodic and acidic crystalline lamellar magadiite adsorbents for removal of methylene blue from aqueous solutions. Kinetic and equilibrium studies, Sep. Sci. Technol. 45 (2010) 129–141.
[45] J.C.P. Vaghetti, E.C. Lima, B. Royer, B.M. da Cunha, N.F. Cardoso, J.L. Brasil, S.L.P. Dias, Pecan nutshell as biosorbent to remove Cu(II), Mn(II) and Pb(II) from aqueous solutions, J. Hazard. Mater. 162 (2009) 270–280.
[46] M.I. El-Khaiary, G.F. Malash, Y.S. Ho, On the use of linearized pseudo-second-order kinetic equations for modeling adsorption systems, Desalination 257 (2010) 93–101.
[47] M.I. El-Khaiary, G.F. Malash, Common data analysis errors in batch adsorption studies, Hydrometallurgy 105 (2011) 314–320.
[48] A.H. Chen, S.M. Chen, Biosorption of azo dyes from aqueous solution by glutaraldehyde-crosslinkedchitosans, J. Hazard. Mater. 172 (2009) 1111–1121.
[49] N. Ertugay, Y.K. Bayhan, The removal of copper (II) ion by using mushroom biomass (Agaricusbisporus) and kinetic modelling, Desalination 255 (2010) 137–142.
[50] L.G. da Silva, R. Ruggiero, P.M. Gontijo, R.B. Pinto, B. Royer, E.C. Lima, T.H.M. Fernandes, T. Calvete, Adsorption of Brilliant Red 2BE dye from water solutions by a chemically modified sugarcane bagasse lignin, Chem. Eng. J. 168 (2011) 620–628.
[51] S. Chatterjee, T. Chatterjee, S.R. Lim, S.H. Woo, Effect of the addition mode of carbon nanotubes for the production of chitosan hydrogel core–shell beads on adsorption of Congo red from aqueous solution, Bioresour. Technol. 102 (2011) 4402–4409.
[52] R. Liu, B. Zhang, D. Mei, H. Zhang, J. Liu, Adsorption of methyl violet from aqueous solution by halloysite nanotubes, Desalination 268 (2011) 111–116.
[53] P. Leechart, W. Nakbanpote, P. Thiravetyan, Application of 'waste' wood-shaving bottom ash for adsorption of azo reactive dye, J. Environ. Manage. 90 (2009) 912–920.
[54] M.S. Bilgili, Adsorption of 4-chlorophenol from aqueous solutions by xad-4 resin: isotherm, kinetic, and thermodynamic analysis, J. Hazard. Mater. 137 (2006) 157–164.
[55] S. Nethajia, A. Sivasamya, G. Thennarasu, S. Saravanan, Adsorption of Malachite Green dye onto activated carbon derived from *Borassusaethiopum* flower biomass, J. Hazard. Mater. 181 (2010) 271–280.
[56] V.K. Gupta, R. Jain, S. Malathi, A. Nayak, Adsorption–desorption studies of indigocarmine from industrial effluents by using deoiled mustard and its comparison with charcoal, J. Colloid Interface Sci. 348 (2010) 628–633.
[57] Y. Liu, Y.J. Liu, Biosorption isotherms, kinetics and thermodynamics, Sep. Purif. Technol. 61 (2008) 229–242.
[58] D.D. Asouhidou, K.S. Triantafyllidis, N.K. Lazaridis, K.A. Matis, S.S. Kim, T.J. Pinnavaia, Sorption of reactive dyes from aqueous solutions by ordered hexagonal and disordered mesoporous carbons, Micropor. Mesopor. Mater. 117 (2009) 257–267.
[59] A.E. Agboola, R.W. Pike, T.A. Hertwig, H.H. Lou, Conceptual design of carbon nanotube processes, Clean Technol. Environ. Policy 9 (2007) 289–311.